

A Study on The Performance of Supersonic Cascade with The Nozzle Inlet Boundary

Bong-Gun Shin¹, Soo-In Jeong¹, Kui-Soon Kim², Eun-seok Lee³

1. The graduate school of Aerospace Engineering department of Pusan National University

2. Department of Aerospace Engineering, Pusan National University

3. Korea Aerospace Research Institute

30 Jangejon-dong, Geumjeong-gu, Busan, 609-735, KOREA

aerogod@empal.com

Keywords: Supersonic Turbine, Impulse turbine, Partial admission turbine, Nozzle inlet boundary condition, Fine Turbo

Abstract

In this study, the flow characteristics within supersonic cascades are numerically investigated by using Fine Turbo, a commercial CFD code. Cascade flows are computed for three different inlet conditions : a uniform supersonic inlet condition, a linear nozzle and a converging-diverging nozzle located in front of cascades. The effect of inlet conditions is compared and flow characteristics including shock patterns and shock-boundary layer interaction are analyzed. Also the effect of design parameters such as pitch-chord ratio, blade angle and blade surface curvature on the flow within supersonic cascades are studied.

1. Introduction

Propellant feed system is an essential component of liquid rockets. The system often employs high-pressure turbo-pump system, which is also a crucial part of induced weapons. Therefore, development of turbo-pump system must be preceded to expand the aerospace and defense industries.

Turbo-pump system adopts partial admission axial turbine which drives pump. Partial admission axial turbine often generates very high power output even though it is small and light. So it is widely used for power generation of various flying vehicles. But performance characteristics of partial admission axial turbine are not available while those of general axial turbine are well known by various experimental and computational studies. The turbine of a turbo-pump system is usually operated at supersonic condition due to its high loading characteristics. The flow characteristics of the supersonic turbine are quite different from common turbine. So it is very difficult to estimate the performance or design the turbine well.

In this situation, the investigation of flow characteristics within supersonic cascades is very important for the development of a turbo-pump

system. So the flow characteristics within supersonic cascades are numerically investigated by using Fine Turbo, a commercial CFD code. Cascade flows are computed for three different inlet conditions : uniform supersonic inlet condition, a converging-diverging nozzle and a linear nozzle located in front of cascades. The effect of inlet conditions is compared and flow characteristics including shock patterns, shock-boundary layer interaction are analyzed. Also the effect of design parameters such as pitch-chord ratio, blade angle and blade surface curvature on the flow within supersonic cascades are studied

2. Results and Discussions

2.1 General methodology and its problem

Usually, cascade flows are analyzed with the computational domain as in shown Fig. 1. Boundaries of the domain consist of suction surface, pressure surface, inlet, outlet and periodic conditions. Sometimes, the inflow condition of a supersonic cascade is affected by the shocks or expansion waves propagated from the leading edge of the blade and is not uniform. In this case, it is very difficult to specify the inlet conditions.

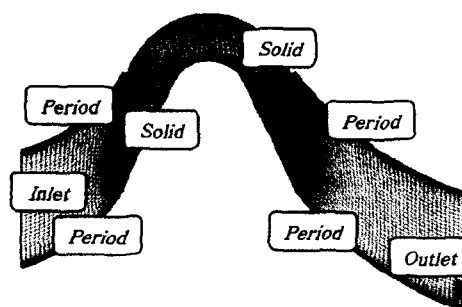


Fig. 1 Geometry & grid system with a far-fild inlet boundary condition

In this paper, numerical analyses have been performed with the far-field boundary condition which is a uniform inlet condition. All computations have

been performed by Fine Turbo, a commercial CFD program. Cascades used in this paper are supersonic cascades designed for a turbo-pump system. A H-type 273×63 grid was used. Velocity, static pressure and static temperature were specified on the inlet boundary and static pressure was enforced on the outlet boundary. And the 3 level multi-grid method was applied to reduce computation time.

Table 1. Computational results of far field inlet boundary condition

the specified inlet boundary values		the computed inlet boundary values
$\beta_1=15.0^\circ$	$M_1=2.563$ $T_1=832K$ $P_1=0.17Mpa$	$M_1=2.563 / \beta_1=15.68^\circ$ $T_1=902K / P_1=0.31Mpa$
$\beta_1=16.89^\circ$		$M_1=2.066 / \beta_1=16.8^\circ$ $T_1=957K / P_1=0.45Mpa$
$\beta_1=20.0^\circ$		$M_1=2.561 / \beta_1=15.68^\circ$ $T_1=1205K / P_1=2.03Mpa$

Table 1. shows the computational results with a far-field inlet condition. The computed inlet boundary values are shown to be different from those of the specified values. The initially specified inlet boundary values were changed because shocks or expansion waves originated from leading edge of blade propagate into inlet boundary and affect the inlet flows. This means that the flow and performance analyses at intended inlet boundary values can't be accomplished.

So, a linear nozzle or a converging-diverging nozzle are located in front of cascades to resolve the non-uniform inlet conditions and the results are compared with those of uniform boundary conditions.

2.2 The inlet condition with linear nozzle or converging-diverging nozzle

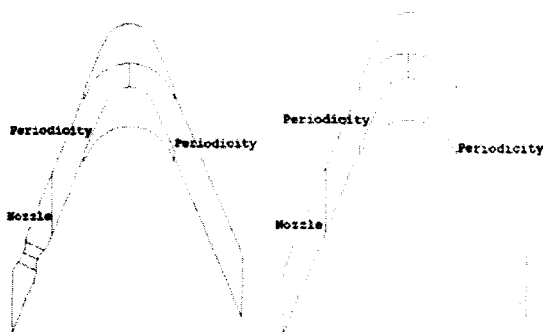


Fig. 2 Inlet condition with converging-diverging nozzle and linear nozzle

The computations at intended inlet condition can not be accomplished due to the change of inlet

condition during computation. So, in this study, the numerical analyses have been performed with a linear nozzle or a converging-diverging nozzle located in front of cascades as shown in Fig. 2.

The area ratio and the direction of the converging-diverging nozzle and the linear nozzle were designed to produce the desired supersonic flows at the exit plane of the nozzle. And the gap between the nozzle exit and cascade blade was deduced from a real turbine.

2.3 The effect of inlet boundary conditions

This study performed numerical analyses for three different inlet conditions, a far-field inlet condition, a inlet condition with a linear nozzle and with a converging-diverging nozzle, to analyze the flow characteristics including shock pattern and shock-boundary layer interaction. And the results were compared with the experimental results of C. D. Colclough⁽¹⁾ and J. J. Cho⁽⁷⁾ to study the effect of the inlet boundary condition with a linear nozzle or a converging-diverging nozzle.

First, the numerical results were compared with the experimental results of C. D. Colclough.

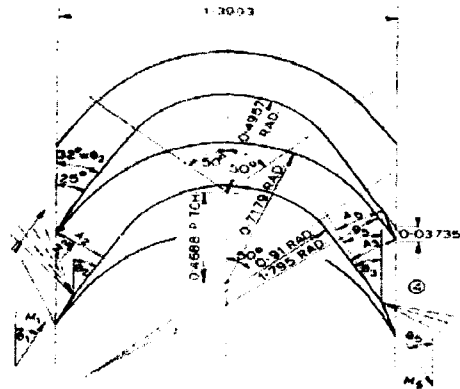
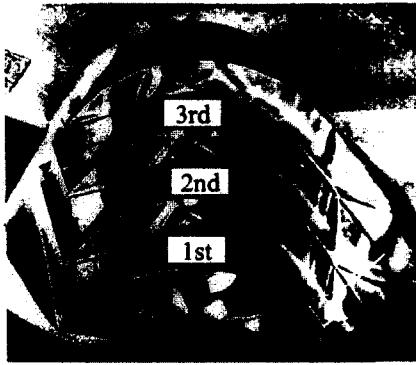
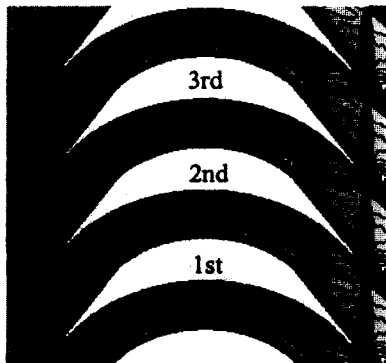


Fig. 3 Supersonic blade profile : Colclough's cascade

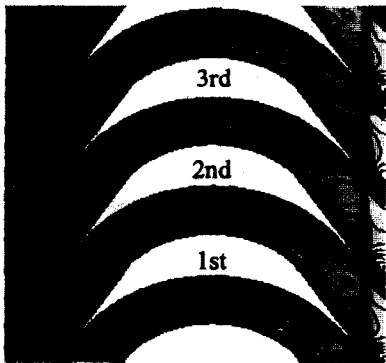
C. D. Colclough had performed the experiment about the flow through supersonic cascades with the wind tunnel which produces Mach number of approximately 1.5 and 1.3. The cascade was designed to satisfy the design condition that was a channel entrance Mach number of 1.366 and turning angle of 116°. The blade is shown in Fig. 3 and consisted simply of straight lines and circles. The wind tunnel supplied 0.75 lb/s of air at 66psi. Computations have also been performed for the corresponding cascade with the 317×77 H-type grid. The linear nozzle and the converging-diverging nozzle were designed and located to make the flow Mach number of 1.5, +9 degree incidence and 66 psi pressure at the exit of nozzle.



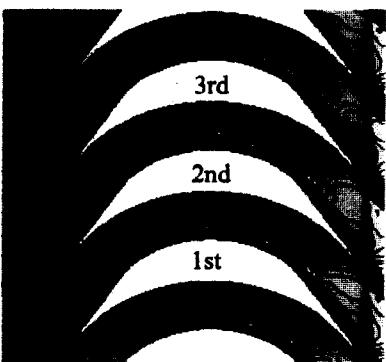
(a) Schlieren image of experiment



(b) Mach contours for far-field inlet condition



(c) Mach contours for linear nozzle inlet condition



(d) Mach contours for converging-diverging nozzle inlet condition.

Fig. 4. Experimental and computational results at +9 degree incidence and Mach 1.5

Fig. 4 (a) shows the Schlieren image of C. D. Colclough for +9 degree incidence and Mach number of 1.5. A weak detached shock wave caused by a slight bluntness is observed around the leading edge of 1st blade. And the second shock wave attached to the leading edge is also discernible on the suction side. The leading edge shock wave from 2nd blade pass through the passage then reflects off the suction surface. And a small separation bubble is observed at about 35 percent of the chord on the suction surface caused by shock-boundary layer interaction.

Fig. 4 (b) shows Mach number contours computed with far-field inlet boundary condition. The computed inlet values are changed from +9 degree incidence and Mach 1.5 (Mach number of 1.5) to +1.5 degree incidence and Mach 1.575. The decrease of incidence angle made the oblique shocks formed at leading edge to be much weaker than those of experiment. The shocks are immediately disappeared by the expansion waves which are generated at 5 percent of the chord on suction surface. The compression waves are observed at the start of pressure surface, pass into channels and are bent by the designed expansion waves which are generated at 30 percent of the chord on the suction surface. Contrary to experiment, computation with far-field inlet boundary condition couldn't catch the separation bubble.

Fig. 4 (c) shows Mach number contours computed with inlet boundary condition with a linear nozzle, and Fig. 4 (d) shows that with a converging-diverging nozzle. The two results are very similar including the flows at exit plane of nozzle. The oblique shocks in the present results are a little different with that in experiment. The difference seems to be caused by the expansion waves attached at the end of the nozzle. Cascades were located in the back of nozzle due to the application of the periodic condition, while cascades in the experiment were located in the nozzle. For that reason, the expansion waves are formed at the end of nozzle and affected the flow entering into channel. Despite of the difference, the characteristics of the flow including the shock and the flow separation are very similar to those of experiment. The oblique shocks are propagated from the leading edge of blades and bent by the designed expansion wave formed at from 30 percent of the chord on suction surface. And the flow is also separated at the 35 percent of the chord on suction surface. The oblique shocks propagated from the leading edge of the 1st and 2nd blade are reflected from the nozzle wall as the experiment.

Comparing the flow characteristics including the flow separation and the shock patterns, the results of inlet boundary condition with nozzle is more accurate than that of far-field inlet boundary condition.

The numerical analyses were also compared with the experimental results of J. J. Cho.

J. J. Cho had performed the experiment with a small supersonic wind tunnel. The wind tunnel was driven by nitrogen gas. The gas entered the nozzles with a total pressure of 110 psi or 200 psi, a total temperature of 293K. Static pressure at exit of test section was atmospheric pressure. The area ratio of supersonic nozzle used in the experiment was 1.687 to produce the Mach number of 2.0 at the exit of nozzle.

Fig. 5 shows the profile of cascade used in the experiment. Each surface of the cascade consists of an arc and two straight lines with circular leading edges. Chord length of the blade is 13.66mm and the ratio of pitch to chord is 0.7.

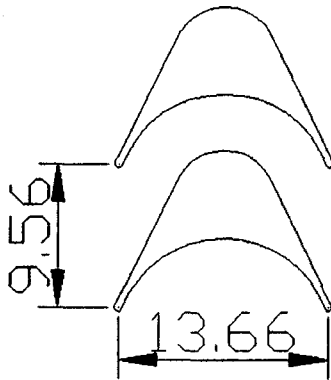
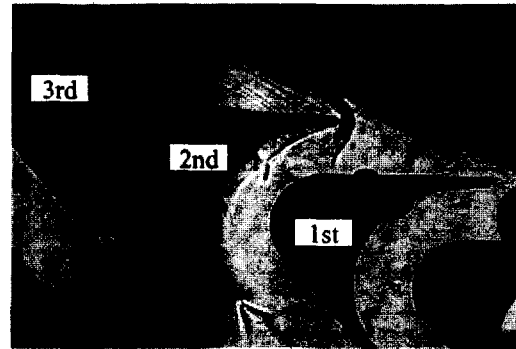


Fig. 5 Supersonic Cascade Profile

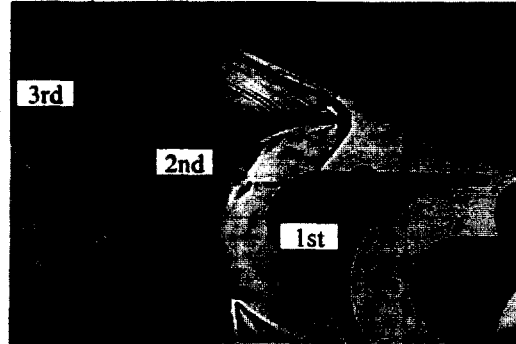
Fig. 6 shows the Schlieren photographs for total inlet pressure of 110 psi and 200 psi. The detached shocks are propagated from leading edge of 2nd and 3rd blades and offset by the expansion waves which are formed at 40 percent of the chord on suction surface. The flows seems to be separated are clearly observed around leading edge of 2nd blade along the pressure surface and at 40 percent of the chord on the suction surface of 2nd blade.

Computations have also been performed for the above experiment.

Fig. 7 shows the computation domains for each inlet condition. Fig. 7 (a) is that with a uniform flow inlet condition. (b) for inlet condition with a linear nozzle. (c) for inlet condition with a converging-diverging nozzle. Here, inlet boundary values of far-field inlet boundary condition and inlet boundary condition with a linear nozzle are specified as the intended inlet values, Mach number of 2.0 and atmosphere pressure. And a converging-diverging nozzle is designed to produce the same flow at exit of nozzle as the inlet boundary values of inlet boundary condition with a linear nozzle.



(a) Inlet total pressure : 110psi



(b) Inlet total pressure : 200psi

Fig. 6 Schlieren image of experimental results

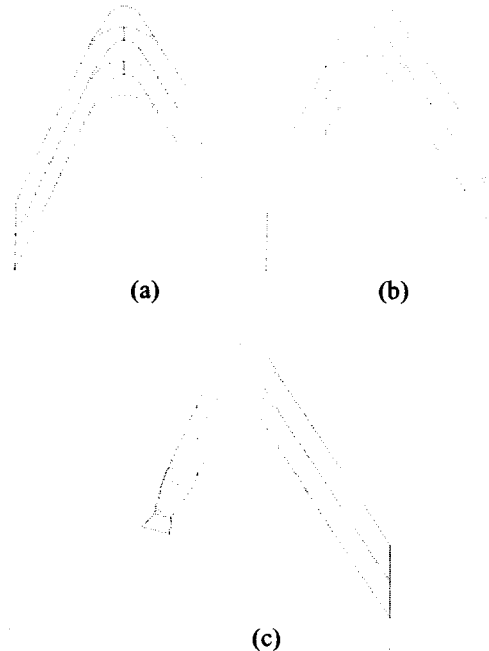


Fig. 7 Geometric conditions for four different inlet conditions

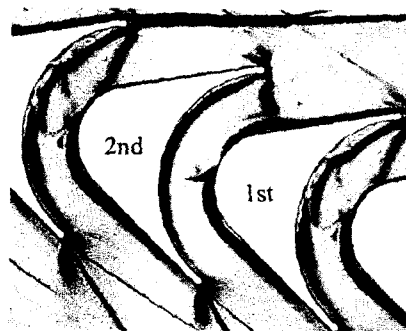
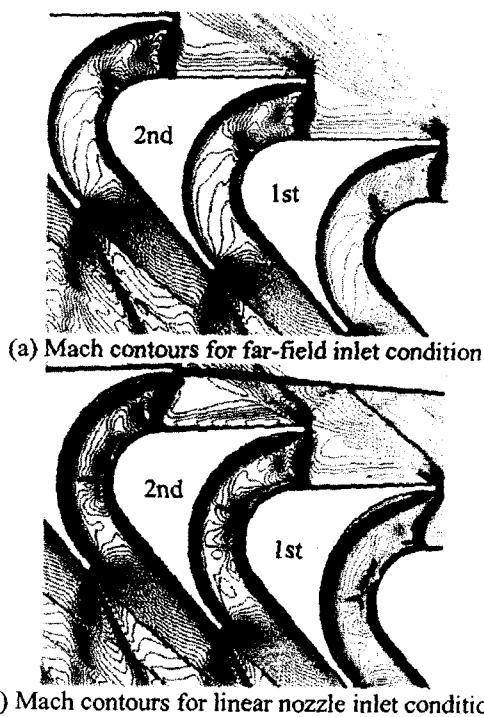
Fig. 8 (a) shows Mach contours computed with far-field inlet boundary condition. Computed inlet values are also changed from the flow of flow angle of 66 and Mach number of 2.0 to that of flow angle of 62.33 and Mach number of 1.67. The change of inlet values causes the oblique shock to be much weaker than that

of the experimental results as shown in Fig. 6. A separation bubble on suction surface, which was clearly observed in the experiment, is hardly observed in this result. But the separation bubble is clearly formed around at leading edge and propagated along the pressure surface. The normal shock is formed at the center of the chord on the suction surface.

Fig. 8 (b) shows Mach number contours computed with a linear nozzle, and Fig. 8 (c) shows that with a converging-diverging nozzle. The detached shocks propagated from leading edge in the computational results are also weaker than that of the experimental result. This seems to be caused not by the change of inlet boundary values as the result of far-field inlet boundary condition, but by the wake attached at the end of nozzle. The wake is caused by the periodic conditions, which affects flows entering into channels.

A separation bubble is formed at 40 percent of the chord on suction surface, which caused by shock-boundary layer interaction. And another separation bubble is formed around the leading edge and propagated along the pressure side. The normal shocks are formed at the center of the chord on the suction surface, which make the flow separation to be more broadened. Comparing the flow characteristics, the results computed with a nozzle are very similar to those of experimental result.

According to the previous comparisons between the numerical results and the experimental results, the computational results for inlet condition with a linear nozzle or a converging-diverging nozzle are more accurate than that of far-field inlet boundary condition.



(c) Mach contours for converging-diverging nozzle inlet condition

Fig. 8 Computational results for inlet total pressure of 200psi

2.4 The study on the performance of supersonic cascade for design parameters

The main geometric parameters, considered in the design of supersonic cascade, are ratio of pitch to chord, blade angle, radius of the surface curvature, and thickness of leading and trailing edge as shown in Fig. 9. And the other computational conditions, such as total pressure and total temperature at the inlet of nozzle, static pressure at the exit of rotor, incidence angle, and velocity of nozzle exit, are confined as intended conditions. So, in this paper, the effect of these on performance of supersonic cascade has analyzed.

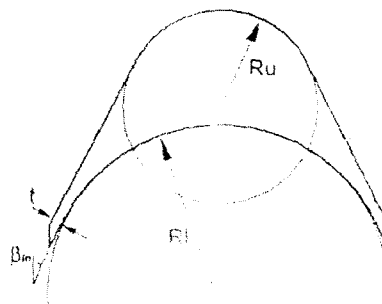


Fig. 9 Design Parameters of supersonic cascade

Fig. 10 shows the computational domain for the computation. The linear nozzle was located in front of cascade to prevent the change of inlet condition, which covers seven channels as design requirement. The gap between the exit of nozzle and blades is 3mm. Periodic condition is applied to simplify the model. The boundary values at the inlet of linear nozzle were specified as a uniform flow of Mach number of 2.0, incidence angle of 3 degree, static pressure of 0.7Mpa, static temperature of 750K. And slip condition was enforced on the nozzle wall. The grid of each channel between blades was H-type (65x433) and that of a

linear nozzle was H-type (449×105) and 3 level multi grid method was used to reduce computation time.

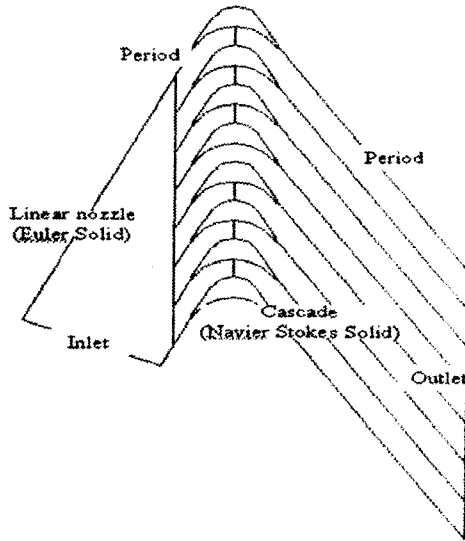


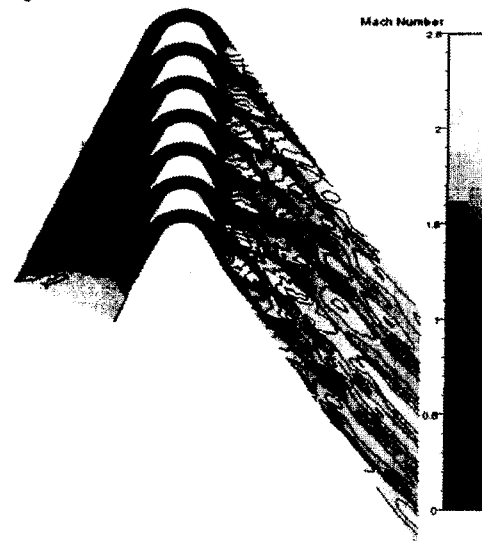
Fig. 10 Geometric system of supersonic cascade

First, the effect of the pitch-chord ratio on the performance has been performed. Fig. 11 (a) shows the Mach number contours of the flow within nozzle and the cascades for the pitch-chord ratio of 0.5. Because the flow area of channels between cascades is not sufficient, the cascades act as the second throat resulting in choking with a normal shock formed in front of the first blade. The inlet flows entering into channels are decelerated to the subsonic flow by the shock. The normal shock create very high loss on performance of the cascade. Because the cascade was designed with a converging-diverging passage, the flows are accelerated, reached to Mach 1.0 at the center of channel, and keep a supersonic flow up to the end of channel. The flow separation isn't observed throughout the channels.

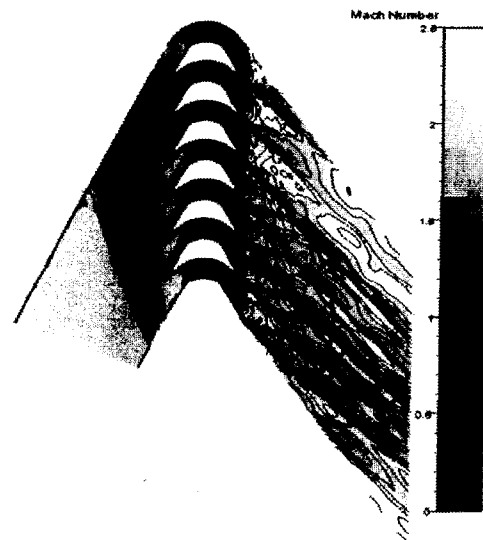
Fig. 11 (b) shows the result for the pitch-chord ratio of 0.637. The flow and shock pattern for pitch-chord ratio of more than 0.55 are different with that for pitch-chord of 0.5, because the enough spill area are provided. The internal flows of nozzle, a uniform flow, are decelerated by the compression waves which are formed at the end of nozzle because the static pressure of the exit of nozzle is lower than that of the axial gap. Oblique shocks are observed at leading edge of from 1st to 5th blade due to the bluntness of the leading edge and the flow at negative incidence. And the shocks are offset by the expansion waves formed at the end of leading edges on the suction surface. Detached shocks are occurred at the leading edge of 6th and 7th blade because of the flow at positive incidence angle caused by the reflected shock. The separation bubble is observed at 30 percent of the chord on the suction surface. Normal shocks are

occurred at the 40 percent of the chord in the channel between 1st and 4th blade. The flows were locally decelerated to subsonic flow by the shocks and then accelerated supersonic again due to diverging-diverging passage.

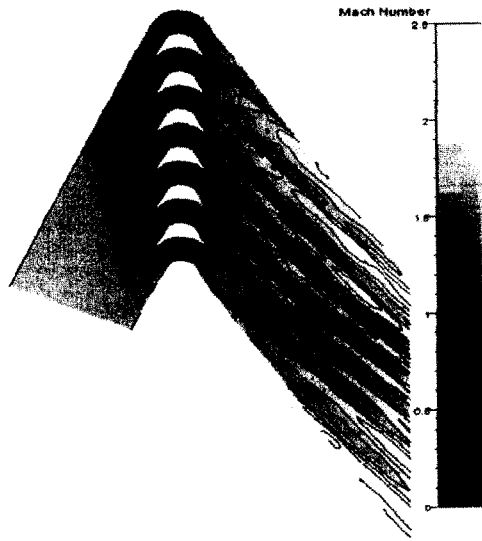
Fig. 11 (c) shows the result for the pitch-chord ratio of 0.8, (d) shows that for the pitch-chord ratio 0.95. The characteristics of the flow and shock pattern are reminiscent of the result for the pitch-chord ratio of 0.637 except the size of the separation bubble and intensity of the shocks. The more the pitch-chord ration is increased, the stronger the intensity of the oblique shocks and the detached shocks are, the more the speed of the flows within cascades are decreased, and the more the sizes of the separation bubble are enlarged.



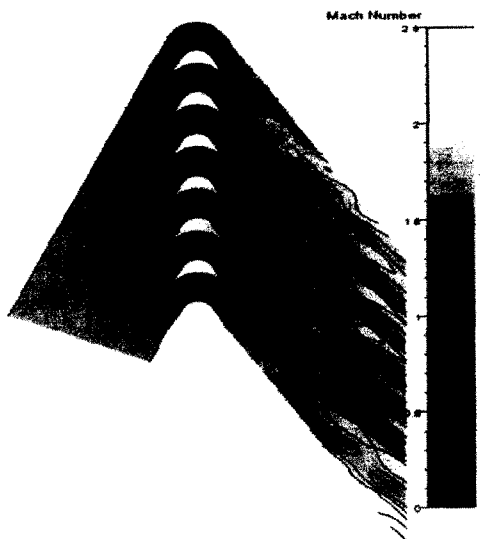
(a) pitch-chord ratio : 0.5



(b) pitch-chord ratio : 0.637



(c) pitch-chord ratio : 0.8



(d) pitch-chord ratio : 0.95

Fig. 11 Mach number contours of the supersonic cascades for pitch-chord ratios.

Fig. 12 shows the distribution of efficiency for each part for the pitch-chord ratio. The more the pitch-chord ratio is increased, the more the efficiency of the inlet part consisting of a linear nozzle and the axial gap between the exit of nozzle and the blade, and the more the circumferential velocity of inlet flow into channels (C_{wi}) is increased. But the more the pitch-chord ratio is increased, the more the efficiency of the flow within cascades is decreased due to the increase of the loss which is caused by the separation bubble, the oblique shocks and the detached shocks.

Fig. 13 show the distribution of turbine power for the pitch-chord ratio, assumed the flow rate is 4.55 kg/s and the axial speed of the blade is 318.87 m/s at 20,000 rpm. The turbine power is minimum at 0.5 pitch-chord ratio because of the choking and the

normal shock. And the more pitch-chord ratio is increased up to 0.8, the more the turbine power is increased because of the increase of the circumferential speed of the inlet flow into channels. But, more than 0.85 pitch-chord ratio, the more pitch-chord ratio is increased, the more the turbine power is decreased because of the increasing loss caused by the separation and the shocks

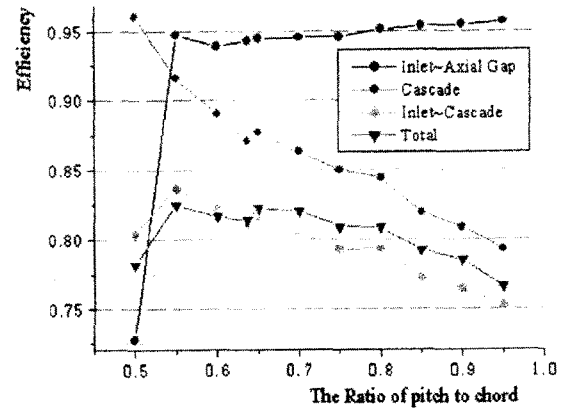


Fig. 12 Distribution of efficiency for each part according to the pitch-chord ratio

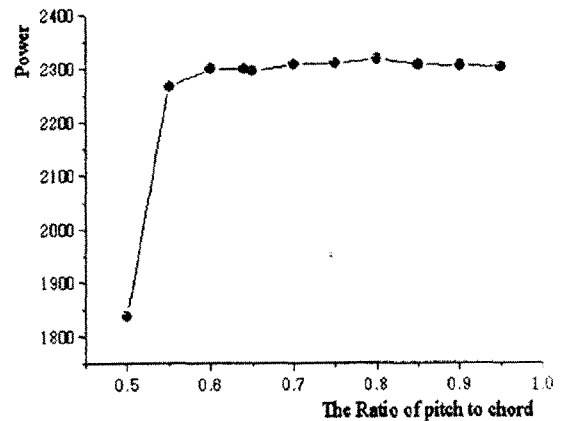


Fig. 13 Distribution of turbine power for the pitch-chord ratio

Finally, the effect of the radius of pressure surface curvature on the performance has been performed.

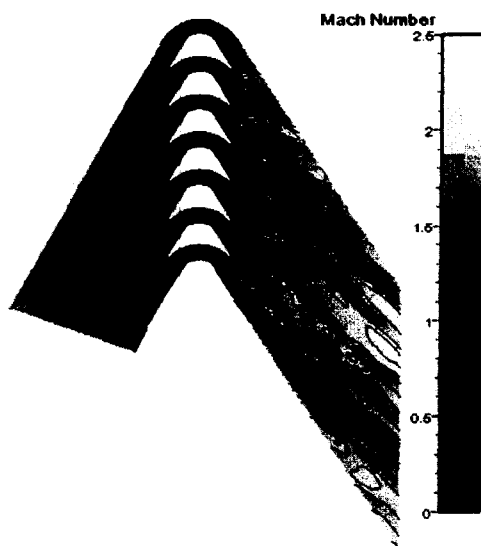
Fig. 14 (a) shows Mach number contours of the flow within nozzle and cascades for the radius of pressure surface curvature of 3.0. The characteristic of the flow and shock patterns is very similar to that for pitch-chord ratio of 0.5. The cascades act as the second throat resulting in choking with a normal shock formed at the inlet of channels except 1st channel due to insufficient spill area. The flows entering into channels are changed to subsonic flow by the shock. The normal shocks create very high loss on performance of cascade. Because the cascade v

designed with a converging-diverging passage, the flow at exit of channel is supersonic.

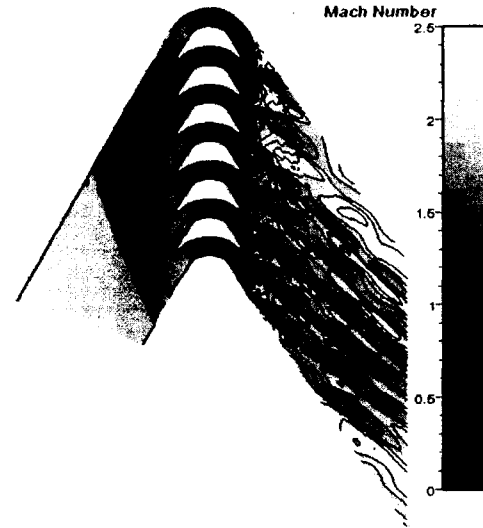
Fig. 14 (b) shows the result for the radius of pressure surface curvature of 3.75, Fig. 14 (c) shows that of 4.25, and Fig. 14 (d) shows that of 5.0. The characteristics of the flow and shock patterns are very similar to that for pitch-chord ratio of more than 0.637. But opposite of the results for the pitch-chord ratio, the more the radius of the curvature is increased, the more the efficiency of the inlet part consisting of a linear nozzle and the axial gap and that of the cascade are decreased, due to the increase of the loss which is caused by the separation bubble, the oblique shocks and the detached shocks except the result for the radius of the pressure surface curvature of less than 3.25.

Fig. 15 shows the distribution of efficiency about each part according to the radius of the pressure surface curvature. The more the radius is increased, the more the efficiency of the inlet part consisting of a linear nozzle and the axial gap between the exit of nozzle and the blade and that of the cascade are decreased, and the more the circumferential velocity of inlet flow into channels (C_{w1}) also decreased except the radius of less than 3.25

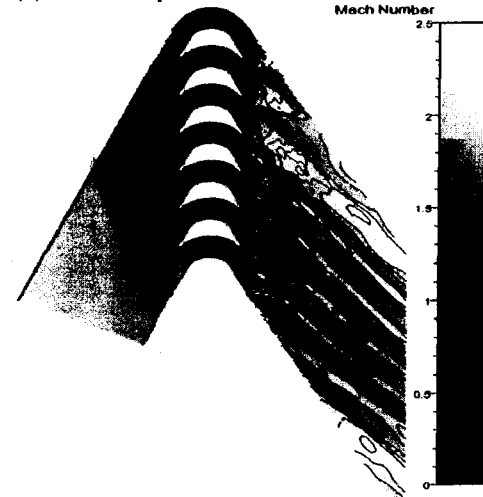
Fig. 16 show the distribution of turbine power for the radius of the pressure surface curvature, assumed the flow rate is 4.55 kg/s and the axial speed of the blade is 318.87 m/s at 20,000 rpm. The turbine power is minimum at the radius of 3.0 because of the choking and the normal shock, and maximum at the radius of 3.75. And the more the radius is increased, more than to 3.75, the more the turbine power is decreased because of the increasing loss caused by the separation and the shocks.



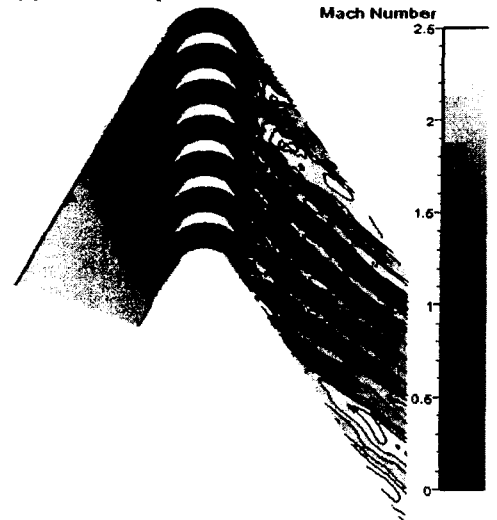
(a) Radius of pressure surface curvature : 3.0



(b) Radius of pressure surface curvature : 3.75



(c) Radius of pressure surface curvature : 4.25



(d) Radius of pressure surface curvature : 5.0

Fig. 14 Mach number contours of the supersonic cascades for the pressure surface curvature

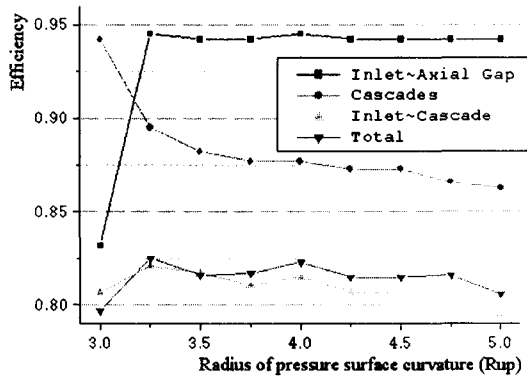


Fig. 15 Distribution of efficiency for each part according to the radius of pressure surface curvature

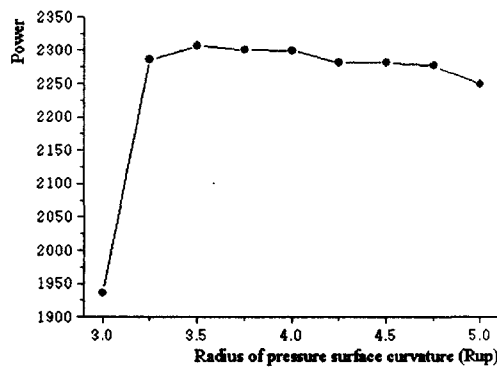


Fig. 16 Distribution of turbine power for the radius of pressure surface curvature

3. Conclusion

This study performed numerical analyses for three different inlet conditions, a far-field inlet condition, an inlet condition with a linear nozzle, and with a converging-diverging nozzle. And the results were compared with the experimental results of C. D. Colclough⁽¹⁾ and J.J. Cho⁽⁷⁾ to study the effect of the inlet boundary condition with a linear nozzle or a converging-diverging nozzle. It is known that the computational results with a linear nozzle or a converging-diverging nozzle are more accurate than that of far-field inlet boundary condition.

The effect of blade geometric parameters, pitch-chord ratio and radius of the pressure surface curvature, on the performance of supersonic cascade has been analyzed. The flow characteristics including the shock pattern for the pitch-chord ratio and the radius of the pressure surface curvature are very similar except the results for the pitch-chord ratio of 0.5 and the radius of the pressure surface curvature of 3.0. The turbine power is shown maximum at the pitch-chord ratio of 0.8 and at the curvature radius of 3.75. And for the pitch-chord ratio of more than 0.85 and the curvature radius of the pressure side of more than 3.5, the more the pitch-chord ratio or the

curvature radius is increased, the more the turbine power is decreased because of the increasing loss caused by the separation and the shocks

References

- 1) Colclough, C. D. : Design of Turbine Blades Suitable For Supersonic Relative Inlet Velocities And The Investigation Of Their Performance In Cascade : Part I - Theory and Design, *Journal Mechanical Engineering Science*, Vol. 8, No 1, 1966, pp. 110-123.
- 2) Colclough, C. D. : Design of Turbine Blades Suitable For Supersonic Relative Inlet Velocities And The Investigation Of Their Performance In Cascade : Part II - Experiments, Results and Discussion, *Journal Mechanical Engineering Science*, Vol. 8, No 2, 1966, pp. 185-197.
- 3) Griffin, L. W, Dorney, D. J : Simulations of the Unsteady Flow Through the Fastrac Supersonic Turbine, *Journal of Turbomachinery*, Vol. 122, April 2000, pp. 225-233.
- 4) Lee, E. S. : Numerical Studies of Geometrical Design Variables for Improvement of Aerodynamic Performance of Supersonic Impulse Turbine, Kari.
- 5) Kiock, A., Lehthaus, F., Baines, N. C. : The Transonic Flow through a Plane Turbine Cascade as Measured in Four European Wind Tunnels, Trans. Of the ASME, *Journal of Engineering for gas Turbines and Power*, Vol. 108, 1986, pp. 277-285.
- 6) Arnone, A, Swanson, R. C. : A Navier-Stokes Solver for Turbomachinery Applications, Trans. Of the ASME, *Journal of Engineering for gas Turbines and Power*, Vol. 115, 1993, pp. 305-313.
- 7) Cho, J. J. : An Experimental Study on The Flow Characteristics of a Supersonic Turbine Cascade, 2004